Received 7 November 2022
Revised 2 April 2023
5 April 2023
Accepted 30 April 2023

An adaptive binary-tree subdivision method for evaluation of nearly singular integrals in 3D BEM

Chuanming Ju
Yantai University, Yantai, China
J. Zhang
Hunan University, Changsha, China
Yudong Zhong
Zhengzhou University of Light Industry, Zhengzhou, China
Xianfeng Du and Jun Li
Yantai University, Yantai, China, and
Baotao Chi
State Key Laboratory of Advanced Design and Manufacturing for Vehicle Body, Hunan University, Changsha, China

Abstract

Purpose – The purpose of this paper is to present an adaptive binary-tree element subdivision method (BTSM) for the evaluation of nearly singular integrals in three-dimensional boundary element method, which can facilitate automatic and high-quality patch generation.
Design/methodology/approach – In this method, the nearly singular element is split into two sub-elements. Each sub-element is then examined to determine if it is to be subdivided based on a specific subdivision criterion. The specific subdivision ensures that those sub-elements far from the source point are sparse. And then those sub-elements in close proximity to the source point are replaced by regular triangular elements.
Findings – With the proposed method, the sub-elements obtained are automatically refined as they approach the projection point, and they are "good" in shape and size for standard Gaussian quadrature. Thus, the proposed method can be used to evaluate nearly singular integrals accurately for cases of different element shapes and various locations of the source point.
Originality/value – Numerical examples for surface elements with various relative locations of the source point are presented. The results demonstrate that the proposed method has much better accuracy and robustness than some other methods.

Keywords Nearly singular integrals, Element subdivision, Binary tree
Paper type Research paper

1. Introduction

An important step in the implementation of the boundary element method (BEM) is the evaluation of various integrals containing kernel functions of the type $1/r^p$, where r is the distance between the evaluation point (also called source point) and the field point, and p represents the order of the singularity (Brebbia *et al.*, 1984; Provatidis, 1998; Gao and Davies, 2000; Qin *et al.*, 2011). These integrals become nearly singular when the source point is very close to the field point. Accurate evaluation of nearly singular integrals plays a key role in

This work was supported by Shandong Provincial Natural Science Foundation of China (ZR2022QA072), National Natural Science Foundation of China (11772125, 11972010 and 12202251), China Postdoctoral Science Foundation (2021M702024).

Engineering Computations
Vol. 40 No. 3, 2023
pp. 718-733

0264-4401
DOI 10.1108/EC-11-2022-0670

many BEM analyses for engineering problems, such as the analysis of thin or shell-like structures (Liu, 1998; Zhang *et al.*, 2011), the contact problems (Aliabadi and Martin, 2000), the sensitivity problems (Zhang *et al.*, 1999) and the displacement around open crack tips (Dirgantara and Aliabadi, 2000). It is well known that traditional Gaussian quadrature rules become inefficient or even inaccurate when applied to evaluate these integrals directly. This is because the value of the integrand varies dramatically as the source point approaches to the integration element.

In order to deal with nearly singular integrals, various methods have been proposed, such as analytical and semi-analytical methods (Niu *et al.*, 2005; Zhou *et al.*, 2008), exponential transformation (Xie *et al.*, 2013, 2014), distance transformation (Qin *et al.*, 2011; Ma and Kamiya, 2002a, b), sin-h transformation (Johnston *et al.*, 2007; Johnston and Elliott, 2005; Gu *et al.*, 2013), quadrature by expansions and other adaptive methods (Greengard *et al.*, 2021). Since analytical integrals do not exist for a generally curved element, the analytical and semi-analytical methods are mainly used for the constant or linear element. As for the above non-linear transformation method, the numerical results are sensitive to the location of the projection point of the source point.

Element subdivision (Gao *et al.*, 2016; Gao, 2010) is one of the most widely used methods for evaluating the nearly singular integral. Zhang *et al.* have developed a spherical element subdivision method (Zhang *et al.*, 2017) for the numerical evaluation of nearly singular integrals in 3D BEM. The sub-elements obtained by this method are "good" in shape and size for standard Gaussian quadrature. However, this method cannot guarantee convergence or successful element subdivision. Thus, we proposed a binary-tree subdivision method (BTSM) whose implementation is simple and robust.

In the proposed BTSM, an element is split into two sub-elements at each step and continues the splitting process recursively until meeting a given terminating criterion. The given terminating criteria can ensure that the sub-elements obtained are automatically refined as they approach the source point. This subdivision algorithm is less cumbersome to implement than other subdivision methods and can guarantee the convergence of the iterative subdivision based on the given terminating criteria. The sub-elements around the projection point of the source point are replaced by new sub-elements which are generated along the radial direction of the sphere centered at the projection point. As a result, each sub-element (also called by patch) is "good" in shape and size for standard Gaussian quadrature, and hence high accuracy can be achieved by a small number of Gaussian sample points.

This paper is organized as follows. The details of the BTSM are discussed in Section 2. In Section 3, results are given to compare the proposed algorithm with other algorithms such as distance transformation method, etc. The paper ends with conclusions in Section 4.

2. The binary-tree subdivision method (BTSM)

2.1 Overall algorithm

A nearly singular element, shown in Figure 1, will be employed to illustrate the binary tree subdivision method. Its shape is an equilateral triangle. The red node is the source point S, and its projection P on the nearly singular element is marked by the black node. The subdivision process of the BTSM is graphically illustrated in Figures 2 and 3.

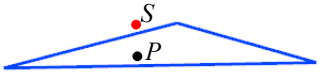

Source(s): Authors work

Figure 1.
The nearly singular element and the source point

The first step of this algorithm is subdivided into sub-elements based on the source point S (see Figure 2(a)). Then the source point is projected to the element. If the projected point is outside the element, we take the point on the element closest to the projection point as a new projection point. Thus, the essence of finding the projection point P of the source point S on the element is to find the point closest to the source point S on the element. The process of obtaining the point closest to an object point on an element is introduced in the reference (Piegl and Tiller, 2010). Three cases are considered: the projection point is inside the element, on the edge of the element and on the vertex of the element. The second step of this algorithm is forming a cavity. Based on this projection, we get a feature sphere (see the yellow sphere in Figure 2(b)). Around this sphere, the cavity forms and is shown in Figure 2(b). The latest is filling the cavity with sub-elements (see Figure 2(c)). The final subdivision result is presented in Figure 2 (d).

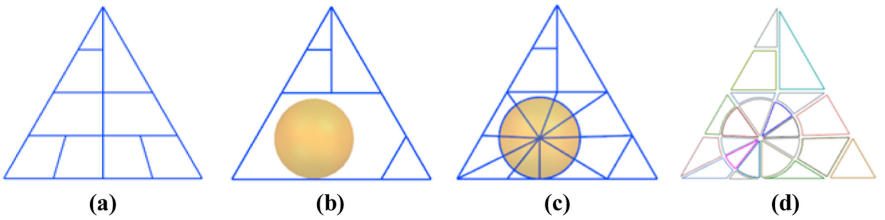

Figure 2.
The subdivision process of the BTSM: (a) initial subdivision result; (b) the formation of a cavity; (c) the cavity filled with sub-elements; (d) final subdivision results

Source(s): Authors work

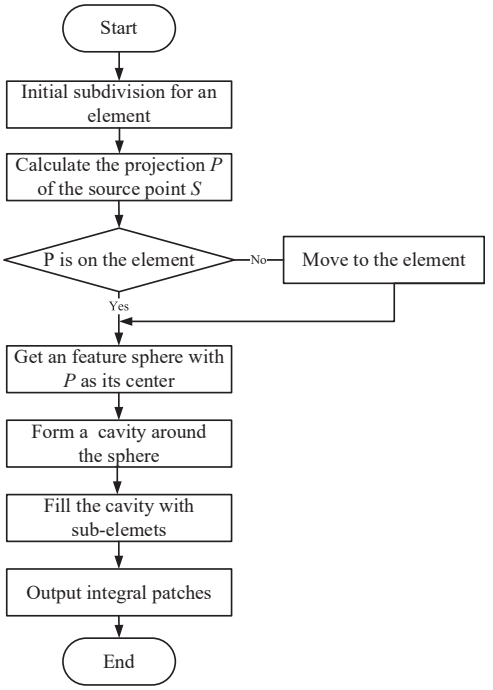

Figure 3.
The flow diagram of the BTSM

Source(s): Authors work

2.2 Details of the algorithm

2.2.1 The initial subdivision of BTSM. In the BTSM, the initial element is subdivided into two sub-elements. Each element is then examined to determine if it is to be subdivided based on a specific subdivision criterion. Different from a quadrilateral element, a triangular element can be divided into two different sub-elements according to its shape. As shown in Figure 4, if the element is a slender triangular element whose height is longer than twice its base, it can be divided into a triangular and quadrilateral sub-element.

The details of the subdivision criterion and process are described below. In Figure 5, S is the source point, C is the center of a circle circumscribed on an element patch, R is the radius of the circumscribed circle and L is the distance from C to S. The coordinates of the center C can be obtained from the parameter coordinates of three vertices of the element patch. The coordinate of the center in 3D physical space can be calculated by the mapping between the 2D parameter space and the 3D physical space. And the radius R and L is the distance between the center and vertex in 3D physical space. If the ratio L/R is smaller than a prescribed value, the patch is assumed to be close enough to the source point to warrant subdivision into two additional patches. Conversely, if the ratio L/R is larger than that prescribed value, the patch is not subjected to further subdivision. The subdivision is further described in the flow diagram shown in Figure 6.

The subdivision criterion ensures that those patches in close proximity to the source point are subjected to subdivision while those far from the source point are not subdivided. And the closer the source point is to the cell, the more patches the element is subdivided into. The source points at different locations relative to the element are shown in Figure 7. And Figure 8 shows the initial subdivision results of the element according to the source points shown in Figure 7.

2.2.2 The formation of the cavity. The formation of the cavity is based on the feature sphere centered at the projection point of the source point. The patches which intersect with the feature sphere, is removed from the subdivisions. Then the cavity is formed. When the projection point is located inside the nearly singular element, the radius of the feature sphere is established as the distance between the source point and the nearest edge. If the projection point is on the boundary of the element, the radius is half of the distance between the

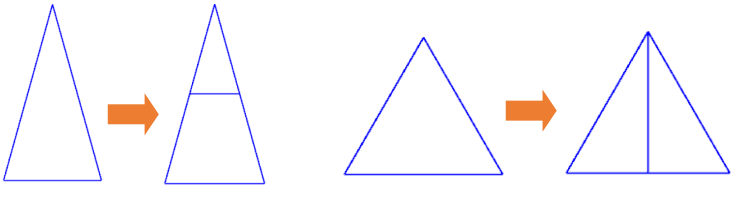

Source(s): Authors work

Figure 4. Two ways to subdivide a triangular element: (a) subdivided into triangular and quadrilateral sub-elements; (b) subdivided into two triangular sub-elements

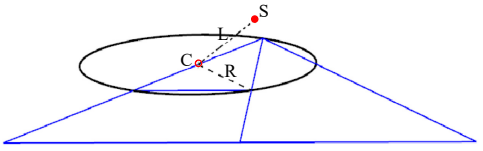

Source(s): Authors work

Figure 5. Distance-based element subdivision criterion

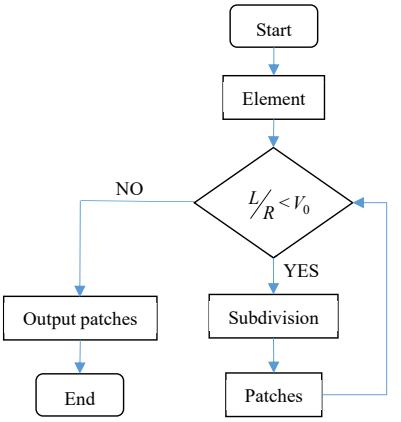

Source(s): Authors work

Figure 6.
Flow diagram of initial subdivision algorithm

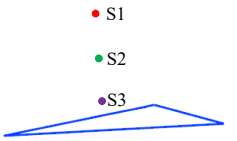

Source(s): Authors work

Figure 7.
The different source points and the nearly singular element

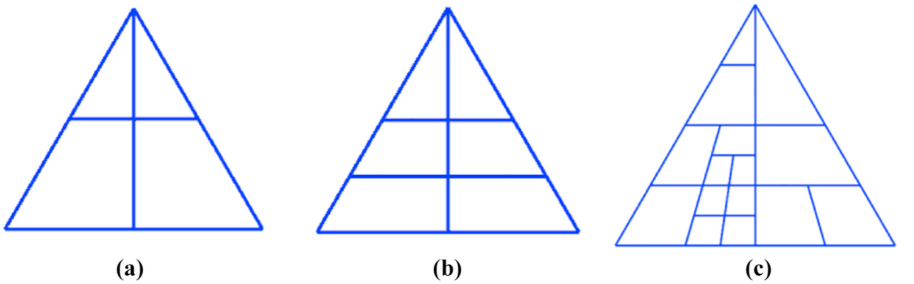

Source(s): Authors work

Figure 8.
The initial subdivision results: (a) the source point S1; (b) the source point S2; (c) the source point S3

projection point and the nearest vertex. Figure 9 shows the formation of cavities around the projection points with different locations.

2.2.3 The formation of the radial patches. The radial patches are composed of external radial patches and internal radial patches. The external radial patches are generated between the cavity and the feature sphere by connecting the vertexes of the cavity and their projection points on the feature sphere. After generating the outer radial patches, the inner radial patches are generated by connecting the projection points on the feature sphere with the projection point of the source point. Figures 10–12 show the formation of radial patches.

3. Numerical examples

To verify the accuracy and efficiency of the BTSM, several computational experiments are implemented to compare its accuracy against other methods, such as the distance transformation technique and sinh transformation method, for triangular and quadrilateral elements. For the purpose of error estimation, a relative error is defined as follows:

$$Error = \left| \frac{I_n - I_e}{I_e} \right| \tag{1}$$

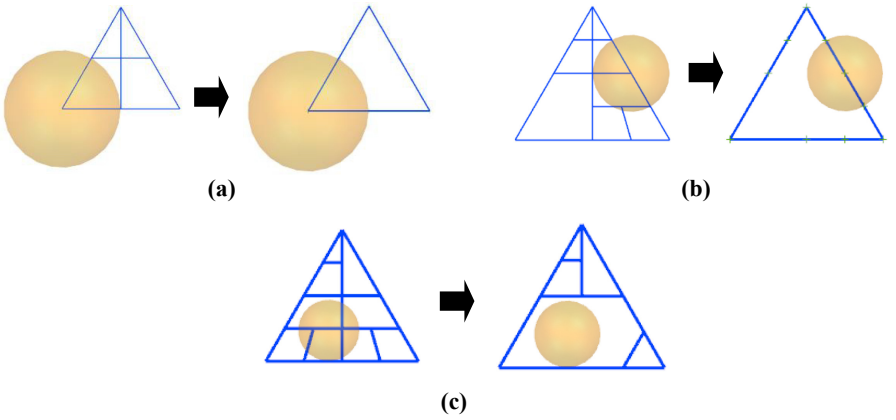

Source(s): Authors work

Figure 9.
The formation of the cavity around the projection points with different locations: (a) the projection point on the vertex of element; (b) the projection point on the edge of element; (c) The projection point inside the element

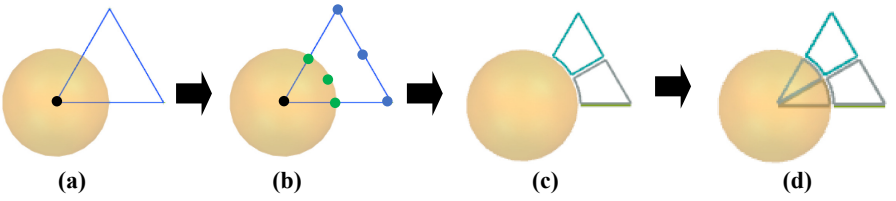

Source(s): Authors work

Figure 10.
For the projection point on the vertex: (a) the cavity; (b) the vertexes of the cavity and their projection points on feature sphere; (c) the external patches; (d) the internal patches

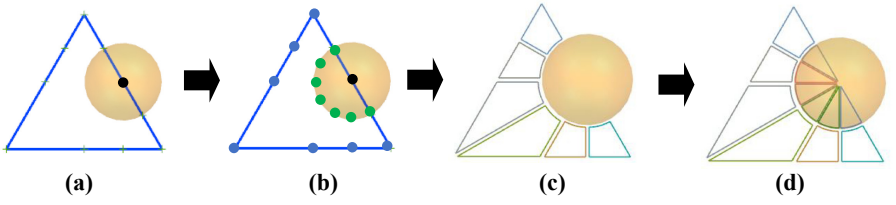

Source(s): Authors work

Figure 11.
For the projection point on the edge: (a) the cavity; (b) the vertexes of the cavity and their projection points on feature sphere; (c) the external patches

where I_n and I_e are the numerical approximation and exact solution of the integral, respectively. For all cases, the following weakly singular integral is considered:

$$I(\xi) = \int_S \frac{1}{|x-\xi|} dS(x) . \tag{2}$$

In all numerical examples, the number of Gaussian sample points and the relative errors of different methods are listed. "A" represents the distance transformation technique. "B" and "C" are the sinh transformation method and the sinh plus sigmoidal transformation method, respectively. The serendipity patch (Zhong *et al.*, 2016) is used in the proposed method. The patch obtained by our method becomes arc-shaped according to the location of the source point. The number of Gaussian points m is determined by (Gao and Davies, 2000; Bu and Davies, 1995; Lachat and Watson, 1976)

$$m = -\frac{1}{10}\ln\left(\frac{e}{2}\right)\sqrt{\frac{2}{3}p+\frac{2}{5}}\left[\left(\frac{8L}{3R}\right)^{\frac{3}{4}}+1\right] \tag{3}$$

where p represents the order of the singularity ($p = 1$), e denotes the error tolerance, L is the length of the patch in the integral direction and R is the minimum distance from the source point to the boundary element.

3.1 Nearly singular integration on triangular element examples

In the first example, the numerical results of the binary-tree subdivision method (BTSM) and other methods for a triangular element are presented. The vertex coordinates of the triangular element are (0, 0, 0), (10, 0, 0), (20, 10, 0) in the physical coordinate system. The source points are uniformly collocated along two lines as shown in Figure 13 with

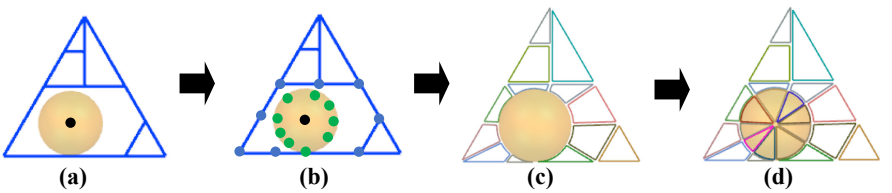

Figure 12.
For the projection point inside the element: (a) the cavity; (b) the vertexes of the cavity and their projection points on feature sphere; (c) the external patches; (d) the internal patches

Source(s): Authors work

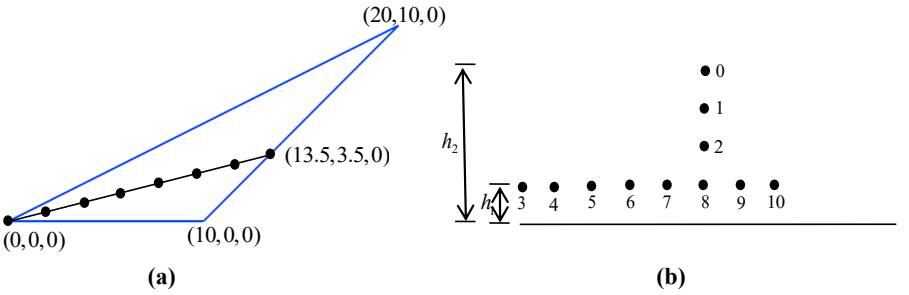

Figure 13.
The triangular element and locations of the source points: (a) top view of the element and the source points; (b) front view of the element and the source points

Source(s): Authors work

h1 = 0.0001, h2 = 0.0045. The source points are numbered with Arabic numerals 0–2 (from top to bottom) and 4–10 (from left to right).

Figures 14 and 15 show the element subdivision results for different locations of the source point. It can be seen from these figures that the shape of the patches around the projection point of the source point is always regular, and the patches close to the source point

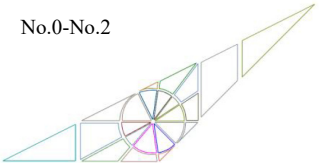

Source(s): Authors work

Figure 14.
Subdivisions for locations of source point moving vertically

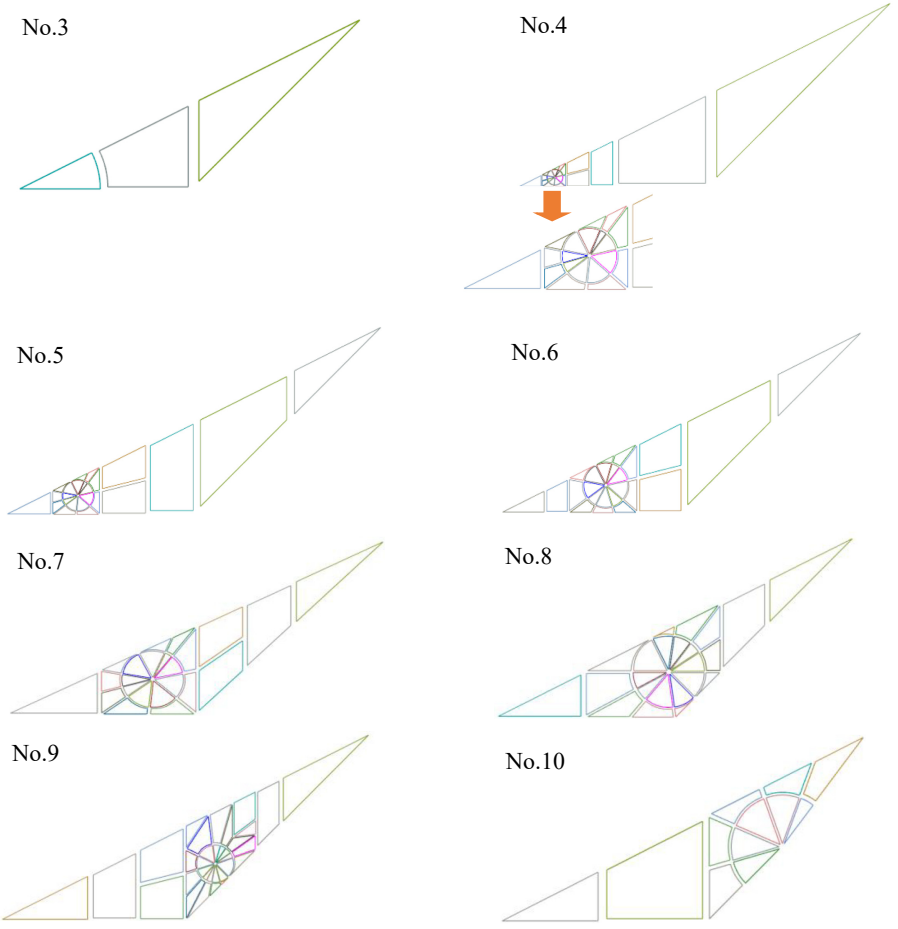

Source(s): Authors work

Figure 15.
Subdivisions for locations of source point moving horizontally

are smaller than those far away from the source point. From Table 1, it can be seen that with similar number of Gaussian points, the accuracy obtained by our method is 2–3 orders of magnitude higher than that by other methods. In comparison with other methods, significantly better accuracy is obtained by the BTSM for various locations of the source point. And the accuracy obtained by our method for all locations of the source point is stable.

3.2 Nearly singular integration on quadrilateral element examples

In this example, the BTSM and other methods are performed on an irregular quadrilateral element. The vertex coordinates of the quadrilateral element are (0, 0, 0), (30, 0, 0), (25, 25, 0), (10, 25, 0) in the physical coordinate system. The source points are uniformly collocated along two lines as shown in Figure 16 with h1 = 0.0001, h2 = 0.0045. The source points are numbered with Arabic numerals 0–2 (from top to bottom) and 4–10 (from left to right). The patches obtained by our method for different locations of source points are shown in Figures 17 and 18. It can be seen that the patches are in "good" shape and size. The number of Gaussian points and the relative errors of different methods are listed in Table 2.

Figures 17 and 18 show the patches in the neighborhood of the projection point are smaller than the distant ones, and the shape of the patches around the projection point is always regular. As Table 2 illustrates, it is usually that the accuracy obtained by our method is higher than that by other methods. Though in a few cases, the distance transform method and the sinh transform method obtain higher precision than our method, the accuracy obtained by our method is stable and acceptable for any position of the source point. Therefore, our method is more suitable for evaluating nearly singular integrals on irregular quadrilateral elements.

3.3 Nearly singular integration on curved element examples

In this example, the BTSM is performed on curved elements. The vertex coordinates of the curved triangular element are (0, 0, 0), (10, 0, 0), (5, 8.6, 0) while the midpoint coordinates of its edges are (5,0,0.8), (7.5,4.3,0.8), (2.5,4.3,0.8). The coordinate of the source points is (4.5.1.72, 1.0161). The patches obtained by our method for the source point are shown in Figure 19(a). And the vertex coordinates of the curved quadrilateral element are (0,0,0), (10,0,0), (10,10,0), (0,10,0) while the midpoint coordinates of its edges are (5,0,0.8), (10,5,0.8), (5,10,0.8), (0,5,0.8). The coordinate of the source points is (5,2.5, 1.4001). The patches obtained by our method for the source point are shown in Figure 19(b). The number of Gaussian points and the relative errors of different methods are listed in Table 3.

	Number of Gaussian points				Relative error			
Source point	A	B	C	Our method	A	B	C	Our method
0	363	363	384	343	7.5486e-2	7.5509e-2	7.6112e-2	4.3086e-3
1	363	363	384	343	7.5313e-2	7.5339e-2	7.5949e-2	2.7365e-3
2	363	363	384	343	7.5188e-2	7.5210e-2	7.5809e-2	1.3925e-3
3	363	363	384	343	7.5108e-2	7.5121e-2	7.5697e-2	4.5185e-4
4	100	100	98	96	6.7686e-1	6.7686e-1	6.7711e-1	1.6367e-6
5	300	300	294	299	3.2369e-1	3.2369e-1	2.7993e-1	4.9948e-5
6	300	300	294	286	5.2695e-1	5.2695e-1	6.8729e-1	2.9531e-5
7	300	300	294	277	3.6699e-1	3.6699e-1	5.1611e-1	2.3398e-5
8	243	243	216	245	2.2886e-1	2.2886e-1	4.2373e-1	1.9887e-5
9	192	192	196	216	7.2733e-2	7.2739e-2	5.8960e-3	2.1883e-5
10	363	363	384	376	1.1463e-3	1.1443e-3	1.2553e-2	1.9005e-5

Table 1.
Numerical results on a triangular element

Source(s): Authors work

As can be seen from Figure 19, the BTSM can be implemented on the curved element. And the accuracy obtained by our method is higher than that by other methods. However, the implementation of the subdivision for more irregular curved elements is the focus of future work.

3.4 Examples compared with spherical element subdivision method

In this example, the spherical element subdivision method represented by "D" is performed on a slender quadrilateral element. The vertex coordinates of the quadrilateral element are (0, 0, 0), (10, 0, 0), (10, 1, 0), (0, 1, 0) in the physical coordinate system. The source points are uniformly collocated along the line as shown in Figure 20 with h1 = 0.001. The source points are numbered with Arabic numerals 0–10 (from left to right). The patches obtained by the spherical element subdivision method and our method for different locations of source points are shown in Figures 21 and 22, respectively. The number of Gaussian points and the relative errors of different methods are listed in Table 4.

It is worth noting that the spherical element subdivision method, proposed by us, has been integrated into the simulation software (called "5aCAE") developed by our team. As can be seen from Table 4, the spherical element subdivision method can provide much better accuracy and efficiency than the BTSM and other methods. However, the spherical element subdivision method cannot guarantee convergence or successful element subdivision. When the spherical element subdivision method is invalid, the BTSM proposed in this paper is employed in 5aCAE to evaluate the nearly singular integration. Although the computational accuracy of BTSM is not as good as that of the spherical element subdivision method, the subdivision algorithm is stable and has higher accuracy compared to other methods.

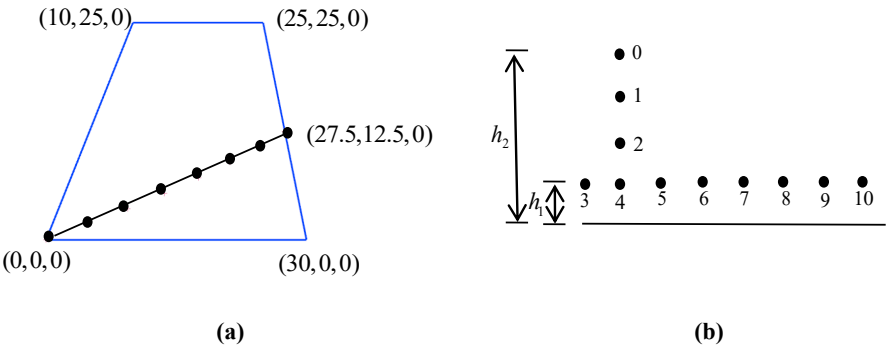

Source(s): Authors work

Figure 16. The quadrilateral element and locations of the source point: (a) top view of the element and the source points; (b) front view of the element and the source points

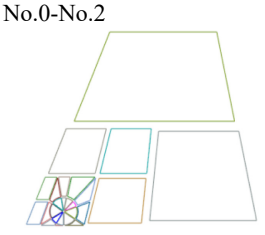

Source(s): Authors work

Figure 17. Subdivisions for locations of source point moving vertically

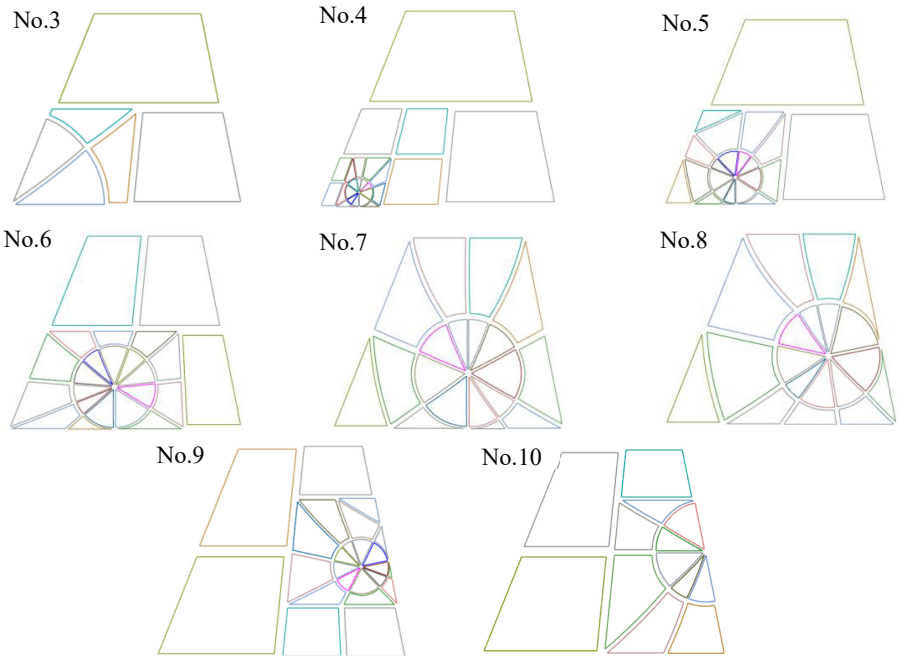

Figure 18.
Subdivisions for locations of source point moving horizontally

Source(s): Authors work

Source point	Number of Gaussian points A	B	C	Our method	Relative error A	B	C	Our method
0	324	324	288	316	2.0029e-4	9.2621e-5	6.3403e-4	1.6698e-3
1	324	324	288	316	1.9992e-4	1.0580e-4	4.6571e-4	1.0264e-3
2	324	324	288	316	1.9892e-4	1.3075e-4	3.2261e-4	5.0263e-4
3	324	324	288	316	1.9849e-4	1.6695e-4	2.8257e-4	1.4430e-4
4	162	162	196	169	4.4654e-5	1.2177e-5	3.4133e-5	2.7139e-7
5	324	324	288	316	1.8429e-4	1.9548e-4	9.3478e-4	1.7332e-5
6	256	256	288	248	5.2695e-5	5.2695e-6	6.8729e-4	2.9531e-6
7	256	256	288	262	3.9920e-5	1.0338e-5	5.6127e-5	1.1727e-6
8	196	196	200	191	2.1036e-4	7.6994e-5	1.9377e-3	3.3240e-6
9	196	196	200	181	1.7155e-4	6.6603e-5	1.3232e-3	1.3108e-5
10	324	324	288	289	4.9894e-7	1.3212e-6	2.6313e-4	2.7910e-6

Table 2.
Numerical results on a quadrilateral element

Source(s): Authors work

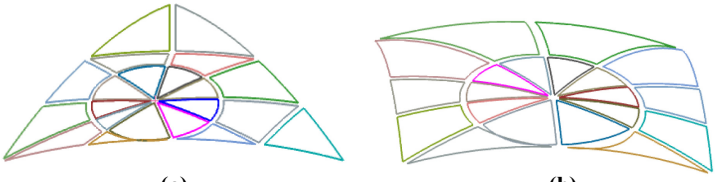

(a) (b)

Source(s): Authors work

Figure 19. Subdivision for curved elements: (a) triangular element; (b) quadrilateral element

Curved element	Source point	Gaussian points number A	B	C	Our method	Relative error A	B	C	Our method
triangle	(4.5,1.72, 1.0161)	192	192	216	199	5.5548e-1	5.6044e-1	9.7894e-1	2.3101e-5
quadrilateral	(5,2.5, 1.4001)	196	196	200	206	1.9640e-4	1.1152e-4	2.6483e-3	2.9899e-5

Source(s): Authors work

Table 3. Numerical evaluation of nearly singular integral for curved elements

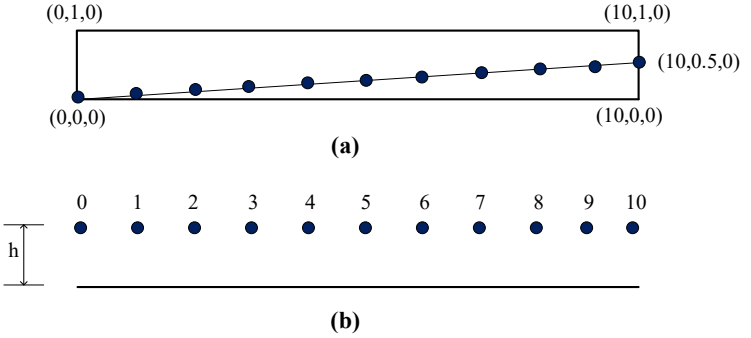

Source(s): Authors work

Figure 20. The slender quadrilateral element and the locations of the source point: (a) Top view of the element and the source points; (b) Front view of the element and the source points

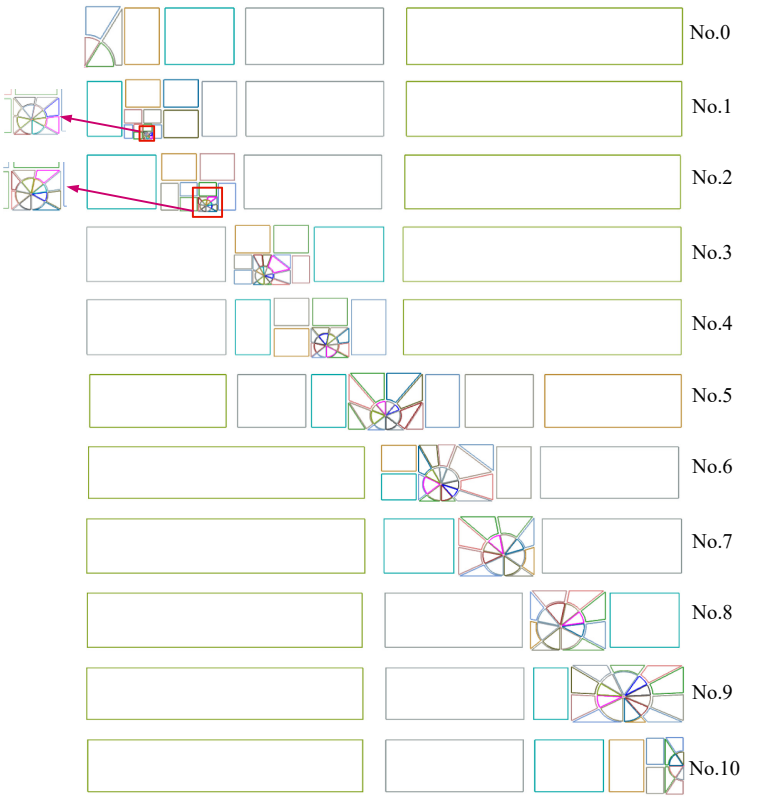

Source(s): Authors work

Figure 21.
Patches obtained by the BTSM for different locations of the source points

4. Conclusions and future work

This paper presented a BTSM for the evaluation of nearly singular integrals which appears in 3D BEM. By applying the proposed method in the BEM, well-shaped patches and excellent numerical results have been successfully obtained for the evaluation of nearly singular integrals. With this subdivision method, the patches obtained are automatically refined as they approach the projection point, and the resulting subdivision patch distribution is dense close to the projection of the source point and sparse far from it. The patches around the projection of the source point are regular triangular patches, and each patch of the integration element is "good" in shape and size for standard Gaussian quadrature. Therefore, all kinds of nearly singular boundary integrals on elements of any shape and size with arbitrary source point locations related to the element can be evaluated accurately. Numerical examples compared with other methods have been presented to verify the robustness and accuracy of the proposed method. The accuracy obtained by our method is stable and acceptable for any location of the source point. In addition, an extension of our method for high order elements and comparison with more other methods is the focus of our future work.

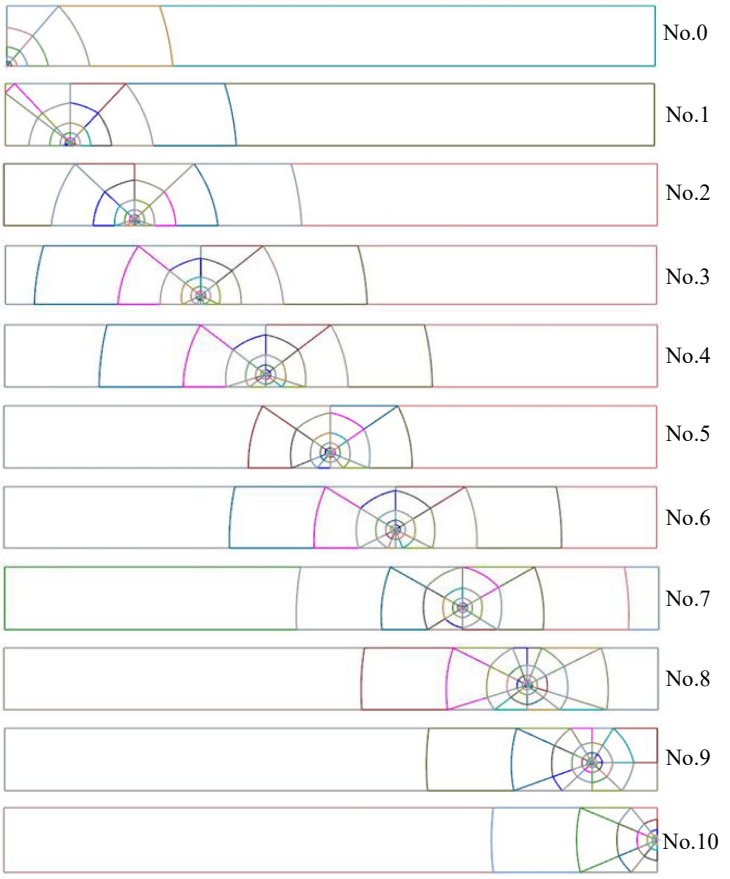

Source(s): Authors work

Figure 22.
Patches obtained by the spherical element subdivision method for different locations of the source points

Source point	Number of Gaussian points A	B	C	D	Our method	Relative error A	B	C	D	Our method
0	98	98	100	175	111	2.9658e-3	2.2404e-4	1.1537e-4	6.3826e-5	2.9658e-3
1	676	676	648	506	469	1.2434e-3	1.2433e-3	6.1853e-3	3.4709e-6	5.0703e-5
2	676	676	648	511	650	4.1515e-3	4.1514e-3	9.9292e-3	9.6752e-6	1.5665e-4
3	676	676	648	522	640	6.4870e-3	6.4868e-3	2.9154e-3	8.9188e-6	9.7302e-4
4	576	576	512	586	576	1.9213e-4	1.9200e-4	1.8060e-3	4.2710e-6	1.8600e-3
5	484	484	512	584	492	1.8304e-2	1.8303e-2	3.8959e-2	1.3552e-6	2.6327e-3
6	484	484	512	586	525	1.0170e-2	1.0171e-2	6.7479e-3	6.5219e-6	3.2850e-3
7	484	484	392	542	449	5.5057e-3	5.5048e-3	3.8604e-2	6.7369e-6	3.8648e-3
8	400	400	392	628	418	8.3938e-3	8.3915e-3	2.5040e-2	6.9944e-6	4.4449e-3
9	484	484	512	584	523	1.1823e-3	1.1832e-3	4.2609e-3	7.9095e-6	5.2019e-3
10	192	192	216	336	192	2.6470e-4	2.7043e-4	4.6551e-5	9.0218e-7	3.6076e-3

Source(s): Authors work

Table 4.
Numerical results on a slender quadrilateral element

References

Aliabadi, M.H. and Martin, D. (2000), "Boundary element hyper-singular formulation for elastoplastic contact problems", *International Journal for Numerical Methods in Engineering*, Vol. 48, pp. 995-1014.

Brebbia, C.A., Telles, J.C.F. and Wrobel, L.C. (1984), *Boundary Element Techniques: Theory Andapplications in Engineering*, Vol. 5, Springer-Verlag, Berlin.

Bu, S. and Davies, T.G. (1995), "Effective evaluation of non-singular integrals in 3D BEM", *Advances in Engineering Software*, Vol. 23 No. 2, pp. 121-128.

Dirgantara, T. and Aliabadi, M.H. (2000), "Crack growth analysis of plates loaded by bending and tension using dual boundary element method", *International Journal of Fracture*, Vol. 105, pp. 27-47.

Gao, X.W. (2010), "An effective method for numerical evaluation of general 2D and 3D high order singular boundary integrals", *Computer Methods in Applied Mechanics and Engineering*, Vol. 199, pp. 2856-2864.

Gao, X.W. and Davies, T.G. (2000), "Adaptive integration in elasto-plastic boundary element analysis", *Journal of the Chinese Institute of Engineers*, Vol. 23, pp. 349-356.

Gao, X.W., Zhang, J.B., Zheng, B.J. and Zhang, C. (2016), "Element-subdivision method for evaluation of singular integrals over narrow strip boundary elements of super thin and slender structures", *Engineering Analysis with Boundary Elements*, Vol. 66, pp. 145-154.

Greengard, L., O'Neil, M., Rachh, M. and Vico, F. (2021), "Fast multipole methods for the evaluation of layer potentials with locally-corrected quadratures", *Journal of Computational Physics: X*, Vol. 10, 100092.

Gu, Y., Chen, W. and Zhang, C. (2013), "The sinh transformation for evaluating nearly singular boundary element integrals over high-order geometry elements", *Engineering Analysis with Boundary Elements*, Vol. 37 No. 2, pp. 301-308.

Johnston, P.R. and Elliott, D. (2005), "A sinh transformation for evaluating nearly singular boundary element integrals", *International Journal for Numerical Methods in Engineering*, Vol. 62 No. 4, pp. 564-578.

Johnston, B.M., Johnston, P.R. and Elliott, D. (2007), "A sinh transformation for evaluating two-dimensional nearly singular boundary element integrals", *International Journal for Numerical Methods in Engineering*, Vol. 69 No. 7, pp. 1460-1479.

Lachat, J.C. and Watson, J.O. (1976), "Effective numerical treatment of boundary integral equations: a formulation for three-dimensional elastostatics", *International Journal for Numerical Methods in Engineering*, Vol. 10 No. 5, pp. 991-1005.

Liu, Y.J. (1998), "Analysis of shell-like structures by the boundary element method based on 3-D elasticity: formulation and verification", *International Journal for Numerical Methods in Engineering*, Vol. 41, pp. 541-558.

Ma, H. and Kamiya, N. (2002), "Distance transformation for the numerical evaluation of near singular boundary integrals with various kernels in boundary element method", *Engineering Analysis with Boundary Elements*, Vol. 26, pp. 329-339.

Ma, H. and Kamiya, N. (2002), "A general algorithm for the numerical evaluation of nearly singular boundary integrals of various orders for two- and three-dimensional elasticity", *Computational Mechanics*, Vol. 29, pp. 277-288.

Niu, Z.R., Wendland, W.L., Wang, X.X. and Zhou, H.L. (2005), "A semi-analytic algorithm for the evaluation of the nearly singular integrals in three-dimensional boundary element methods", *Computer Methods in Applied Mechanics and Engineering*, Vol. 31, pp. 949-964.

Piegl, L. and Tiller, W. (2010), *Non-uniform Rational B-Spline*, Tsinghua University Press, Peking, pp. 163-167.

Provatidis, C. (1998), "A boundary element method for axisymmetric potential problems with non-axisymmetric boundary conditions using fast fourier transform", *Engineering Computations*, Vol. 15, pp. 428-449.

Qin, X., Zhang, J., Xie, G., Zhou, F. and Li, G. (2011), "A general algorithm for the numerical evaluation of nearly singular integrals on 3D boundary element", *Journal of Computational and Applied Mathematics*, Vol. 235 No. 14, pp. 4174-4186.

Xie, G.Z., Zhang, J.M., Huang, C., Lu, C.J. and Li, G.Y. (2013), "Calculation of nearly singular boundary element integrals in thin structures using an improved exponential transformation", *Computer Modeling in Engineering and Sciences*, Vol. 94 No. 2, pp. 139-157.

Xie, G.Z., Zhang, J.M., Dong, Y.Q., Huang, C. and Li, G.Y. (2014), "An improved exponential transformation for nearly singular boundary element integrals in elasticity problems", *International Journal of Solids and Structures*, Vol. 51, pp. 1322-1329.

Zhang, D., Rizzo, F.J. and Rudolphi, T.J. (1999), "Stress intensity sensitivities via hypersingular boundary integral equations", *Computational Mechanics*, Vol. 23, pp. 389-396.

Zhang, Y.M., Gu, Y. and Chen, J.T. (2011), "Boundary element analysis of 2D thin walled structures with high-order geometry elements using transformation", *Engineering Analysis with Boundary Elements*, Vol. 35, pp. 581-586.

Zhang, J., Wang, P., Lu, C. and Dong, Y. (2017), "A spherical element subdivision method for the numerical evaluation of nearly singular integrals in 3D BEM", *Engineering Computations*, Vol. 34 No. 6, pp. 2074-2087.

Zhong, Y.D., Zhang, J.M., Dong, Y.Q., Li, Y., Lin, W.C. and Tang, J.Y. (2016), "A serendipity triangular patch for evaluating weakly singular boundary integrals", *Engineering Analysis with Boundary Elements*, Vol. 69, pp. 86-92.

Zhou, H.L., Niu, Z.R., Cheng, C.Z. and Guan, Z.W. (2008), "Analytical integral algorithm applied to boundary layer effect and thin body effect in BEM for anisotropic potential problems", *Computers and Structures*, Vol. 86, pp. 1656-1671.

Corresponding author
Chuanming Ju can be contacted at: cmju@hnu.edu.cn